Enhanced calcium sensitivity in evolved SARS-CoV-2 strains for fusion and entry

A research project by

Puspangana Singh

Prime Minister Research Fellow (PMRF)

PhD scholar, Lab of Single Molecule Biophysics & Virology

Indian Institute of Technology, Kanpur

Title: Enhanced calcium sensitivity in evolved SARS-CoV-2 strains for fusion and entry

Introduction

With the ongoing pandemic, better intervention strategies are needed in the form of better understanding of the viral entry and fusion landscape. The breakthroughs in vaccine development and therapeutic strategies have been unprecedented in the face of the pandemic, but with the virus mutating at such a fast rate, it is important to get a clear understanding of the entry and fusion of the virus. The SARS-CoV-2 spike glycoprotein has been reported to interact with a number of host cell factors, with ACE2 and TMPRSS2 being the essential factors. However, there are some other indirect interactions of the spike, which have been reported to affect viral infectivity and tropism. A recent report highlighted that another host factor, Neuropilin-1 (NRP1) can also interact with the spike and impact infectivity. With various reports on how different cellular proteins can bind to the spike of SARS-CoV-2, there is a need to pinpoint the exact cellular factors which may be triggering the binding, and subsequently, fusion and entry. There are two major pathways through which coronavirus fusion is supposed to be taking place: the cell membrane pathway, and the endo-lysosomal pathway. A major distinction between the two pathway is the big difference in pHs that the virion would encounter, as different compartments in the cell have different pHs. The pH at the cell membrane is around 7.2-7.4, while the endo-lysosomal pH ranges from pH 4.5-5. Clearly, pH may be one of the factors responsible for coronavirus fusion, the role of which has not been explored till date. There have been reports about how in the pre-fusion structure, SARS-CoV-2 spike RBD exhibits different conformations, however, the effect of pH on the pre-to-post fusion conformational rearrangement of the spike is not clear. Along with pH, there may be other factors in conjunction which may be responsible for fusion. For MERS and SARS-CoV, it has been reported that calcium enhances their infectivity. Hence, calcium may be potentiating infectivity and fusogenicity of SARS-CoV-2. However, an important aspect to keep in mind here is the gradient of calcium concentration which exists in the cell. The cytosolic environment has a relatively low concentration of calcium (~ 10-100 μM), while the endoplasmic reticulum and the lysosomes have a calcium concentration of ~ 400-600 μM. This gradient of calcium concentration in the cell is maintained by various transporters and ion channels.

The pandemic worsened with the fast-paced appearance of new variants. Majority of the mutations have been in the spike glycoprotein, showing that the virus is exploiting the entry and fusion mechanism in order to increase its infectivity. The pandemic started with the wild type variant, after which a single mutation in the spike, D614G, resulted in wide-spread casualties. The spike kept evolving into numerous other variants, with the B.1.315, B.1.1.7 and the B.1.617.2 variants being the most significant worldwide. Out of all the variants present till date, the Delta variant (B.1.617.2) is the most infectious, even when there have been newer variants which are better at immune evasion. With the appearance of the newer variants, it is important to understand the physiological picture which may be responsible for affecting the fusion of different variants.

Objectives

1. To find out the triggers for SARS-CoV-2 spike-mediated fusion in the presence of reported host cell factors (ACE2, TMPRSS2 and NRP1).
2. To understand the role of calcium in spike-mediated fusion to the host cell.
3. To find out any correlation between the variants and calcium concentration dependence.
4. To find out the factor which may bring a pre-to-post fusion conformational change for the SARS-CoV-2 spike.
5. To deduce the major route of entry and fusion used by SARS-CoV-2.

Material and Methods

Production of DiO-labelled lentiviral pseudovirions having SARS-CoV-2 variant spikes

Plasmids encoding different SARS-CoV-2 variant spikes (D614G/B.1.351/B.1.1.7 or B.1.617.2) and a plasmid encoding HIV-1 GagPol were transfected in HEK293T/17 cells using lipofectamine (Invitrogen), in a ratio of 5:5 of Spike:GagPol. HEK293T/17 cells were maintained in DMEM (GIBCO), supplemented with 10% FBS (GIBCO), 2mM L-glutamine (GIBCO) and 100U/mL penicillin/streptomycin (GIBCO) at 37 °C, with 5% CO2, and transfected at 70-75% confluency.

72 hours post-transfection, the supernatant was collected and filtered through a 0.45um filter in order to remove cell debris. Viruses were concentrated in a 10%

sucrose cushion by ultra-centrifugation at 25,000xg for 2 hours. The concentrated pseudovirions were then labelled with 20 μM DiO (Invitrogen) for 2 hours at room temperature in rotation. The labelled pseudovirions were purified using a 6%-30% OptiPrep gradient (Sigma-Aldrich) by centrifugation at 35,000xg for 1 hour. The labelled fractions having the virions were aliquoted and stored at -80 °C for further use.

Liposome preparation

Liposomes with phosphatidylserine (PS) were prepared in a 4:4:0.5:0.1:2 ratio of 1,2, dioleoyl-sn-glycero-3-phosphocholine (DOPC; Avanti Polar Lipids), 1-palmitoyl-2-oleoyl-glycero-3-phosphocholine (POPC; Avanti Polar Lipids), phosphatidylserine (PS; Avanti Polar Lipids), Ni-NTA DGS lipid (Avanti Polar Lipids) and cholesterol (Avanti Polar Lipids). Briefly, the lipids were mixed in chloroform, which was evaporated under a stream of argon gas. The dried lipid film was resuspended in HNE buffer (5mM HEPES, 145mM NaCl; pH 7.5), which was followed by five freeze-thaw cycles. Liposomes of around 100nm were obtained by extruding the homogenized aqueous lipid suspension through a 100nm polycarbonate membrane filter. The freshly-prepared liposomes were coated with histidine-tagged hACE2, NRP1-b1 and hTMPRSS2 in a ratio of 1:1:1 at 37 °C for at least 1 hour in rotation. Liposomes without phosphatidylserine (PS) were prepared in a 4:4:0.1:2 ratio of 1,2, dioleoyl-sn-glycero-3-phosphocholine (DOPC; Avanti Polar Lipids), 1-palmitoyl-2-oleoyl-glycero-3-phosphocholine (POPC; Avanti Polar Lipids), Ni-NTA DGS lipid (Avanti Polar Lipids) and cholesterol (Avanti Polar Lipids).

Virus-liposome lipid mixing assay

DiO-labelled virions with either WT spike or D614G spike were combined with proteo-liposomes (either with or without PS) coated with hACE2, NRP1-b1 and hTMPRSS2. Buffer solution was added in a stop-flow manner to adjust desired pH conditions and DiO fluorescence was followed in a time-based manner. DiO was excited at 488 nm and fluorescence was detected at 515 nm at every second's intervals for 20 minutes in a QuantaMaster fluorescence spectrophotometer 8450 (Horiba). All the fusion experiments were performed at 37 °C by rapid Peltier temperature-controlled sample holder. Data was acquired with the FelixGx software provided by the manufacturer. All the data was analyzed and plotted using MATLAB.

Virus fusogenicity assay

The fusogenicity of the pseudotyped virions was tested by a β-lactamase (BlaM)-based enzymatic assay (LiveBlazer FRET B/G kit, Invitrogen). The pseudoviruses were formed as described above, but with an additional plasmid encoding BlaM, fused to the HIV-1 Vpr protein. Viruses were collected and concentrated as described above and resuspended in phenol red-free DMEM (GIBCO), supplemented with 10% FBS (GIBCO), 2mM L-glutamine (GIBCO) and 100U/mL penicillin/streptomycin (GIBCO). Vero-TMPRSS2 cells were seeded in 96-well plates and incubated with either Lact-C2 or exogenous phosphatidylserine (PS). Lact-C2 diluted in DMEM was used at a final concentration of 100nM, and PS in chloroform diluted in MilliQ water was used at a final concentration of 2.5uM. The virions were then used for infecting HEK293T/17 cells. Spinoculation was done at 3700 rpm at 4 °C. Unbound viruses were removed by washing with HBSS (GIBCO) and resuspending the cells in fresh phenol red-free DMEM. The plate was then incubated at 37 °C for 90 minutes in order to permit viral entry. Cells were then loaded with the substrate, CCF4-AM fluorophore, in presence of probenecid at a final concentration of 2.5 mM. The plate was incubated overnight at 11 °C. The cleavage of CCF4-AM by BlaM was detected using a plate reader (Biotek). The fusogenicity of the virus was calculated as a ratio of blue to green emission.

Incorporation of non-canonical amino acid in the SARS-CoV-2 spike (S*)

A single non-canonical amino acid (ncAA), TCO*, was incorporated into the S2 domain of SARS CoV-2 spike through amber stop codon suppression technology, as described previously. TAG codon was introduced at the position 836 of S2 near the fusion peptide proximal residue (FPPR). Translation to incorporate the ncAA was allowed to proceed through the UAG codons on the mRNA in the presence of an orthogonal tRNA (tRNAPyl), which recognizes the UAG codon. A corresponding aminoacyl-tRNA synthetase (NESPylRSAF) was used which aminoacylates the suppressor tRNA with TCO*, facilitating its incorporation at the 836th position into S, forming S*. The efficiency of amber suppression is limited due to competition of the eukaryotic release factor 1 (eRF1) with tRNAPyl. Expression of the dominant negative eRF1 E55D mutant increased amber suppression efficiency.

HEK293T cells were transfected with plasmids encoding the Spike, TAG-mutated S*, NESPylRSAF/tRNAPyl, eRF1 E55D, and HIV-1 Gag-Pol in a ratio of 2.5:2.5:2.5:1.5:5.

The growth medium was supplemented with 500uM TCO* ncAA (SiChem). At 72 hours post-transfection the virus was harvested by using a 0.45um syringe filter. The virions were concentrated in a 10% sucrose cushion by centrifugation at 25,000xg at 4 C. The concentrated virions were labelled with DSPE-Biotin for 30 minutes in rotation, following which 500μM Cy5 was added. Cy5-labelled virions were purified in a 6%-30% Opti-Prep gradient by centrifugation at 35,000xg for 1 hour. The fractions having the labelled virions were collected.

Fluorescence anisotropy

Cy3-labelled virions were used for anisotropy measurements.

Anisotropy is a measure of the extent of polarization of a fluorophore. The rotational diffusion of a fluorophore, linked to a protein, reflects the local conformational motion of the residue labelled, which is the fusion peptide of the SARS-CoV-2 spike. Hence, fluorescence anisotropy was used to determine whether the fusion peptide of the spike is getting inserted into the liposome membrane or not, in the presence of the triggers indicated.

Anisotropy measurements were done by exciting Cy3 at 532 nm and collecting emission at 570 nm, in a QuantaMaster fluorimeter (Horiba) in presence of polarizers. The G-factors measured for the experiments done and calculated using the lookup table. An integration time of 1 s was used for all the anisotropy experiments. All measurements were done at 37 °C.

FRET assay to find out the pre-to-post fusion conformational transition of the spike

Virions containing either the wild-type spike or the D614G spike variant, each bearing Q836TCO* and G1035TCO* markers, were subjected to labeling using tetrazine-Cy3 (as the donor) and tetrazine-Cy5 (as the acceptor), following the procedure outlined earlier. The QuantaMaster (QM-8450, Horiba) instrument was employed to measure the fluorescence of the donor, employing an excitation wavelength of 532 nm, and the emitted light was collected within the range of 550 nm to 700 nm. Subsequently, these virions, along with proteo-liposomes that included the ACE2, NRP1, and TMPRSS2 receptors, were subjected to an incubation process. Through a stopped flow

technique, a combination of low pH and CaCl2 was introduced, and measurements of the donor fluorescence were taken.

The efficiency of fluorescence resonance energy transfer (FRET) was calculated by contrasting the donor fluorescence in the presence of the acceptor with the donor fluorescence alone, as present within the spike protein of the virions. In instances of high fluorescence resonance energy transfer (High-FRET), there was a reduction in the intensity of donor emission coupled with an elevation in the intensity of acceptor emission. Conversely, low FRET led to heightened donor emission intensity and diminished acceptor emission intensity. The FRET experiments were conducted across a broad range of calcium concentrations (ranging from 100 µM to 10 mM) at a pH of 4.6. All experiments were carried out at a temperature of 37°C.

Results

a. Spike and ACE2, NRP1 & TMPRSS2-mediated membrane fusion is driven by calcium and acidic pH

Reconstitution assays that mimic virus and host cell fusion are important to understand and pinpoint the factors which may be playing crucial role in fusion. Hence, a fluorescence-based fusion assay was designed which consisted of HIV-based pseudovirions tagged with the lipophilic dye DiO, and proteoliposomes. The proteoliposomes had phosphatidylcholine, phosphatidylserine, cholesterol, and a Ni-NTA conjugated lipid. The liposomes were coated with ACE2, TMPRSS2 and NRP1, which are the known host cell factors for the SARS-CoV-2 infectivity (Figure 1).

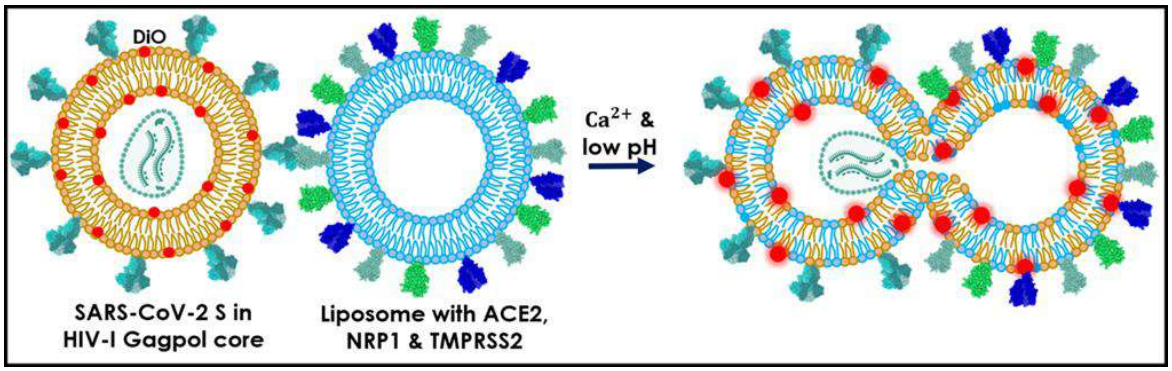

Figure 1: Assay design for the bulk fluorescence reconstitution assay in order to monitor fusion of SARS-CoV-2 pseudovirions with liposomes coated with ACE2, NRP1 and TMPRSS2. Assay has been described in detail in the methods section.

No considerable fusion was observed at pH 7 or pH 6, even with 500 μM calcium present (Figure 2A-D).

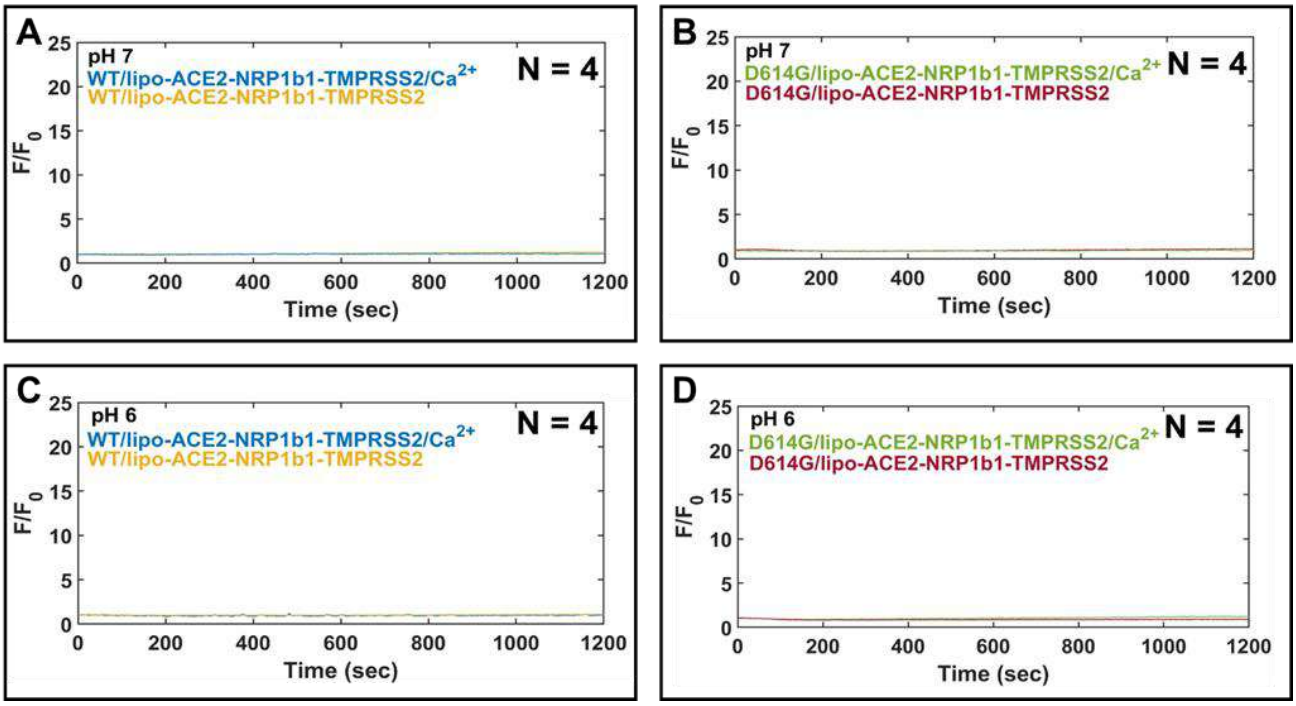

Figure 2: Fluorescence versus time plots for WT (A & C) and D614G (B & D) at pH 7 and pH 6 in presence and absence of calcium.

Significant fusion was observed in presence of calcium when pH was dropped to 5 (Figure 3 A,B). However, the highest fusion was observed for D614G at pH 4.6 and calcium (Figure 3 C,D). With all the three receptors present, the fusion efficiency for D614G was calculated to be around 37%, while that for wild type was calculated to be around 18% (Figure 3E).

Looking at the fusion indices of fusion at pH 4.6 and 500 μM calcium in presence of individual receptors, and when all the receptors are present together, it became evident that the highest fusion efficiency is observed when all the three proteins are present together. Interestingly, D614G showed higher fusion efficiency in all the cases, as compared to the wild type spike (Figure 3F).

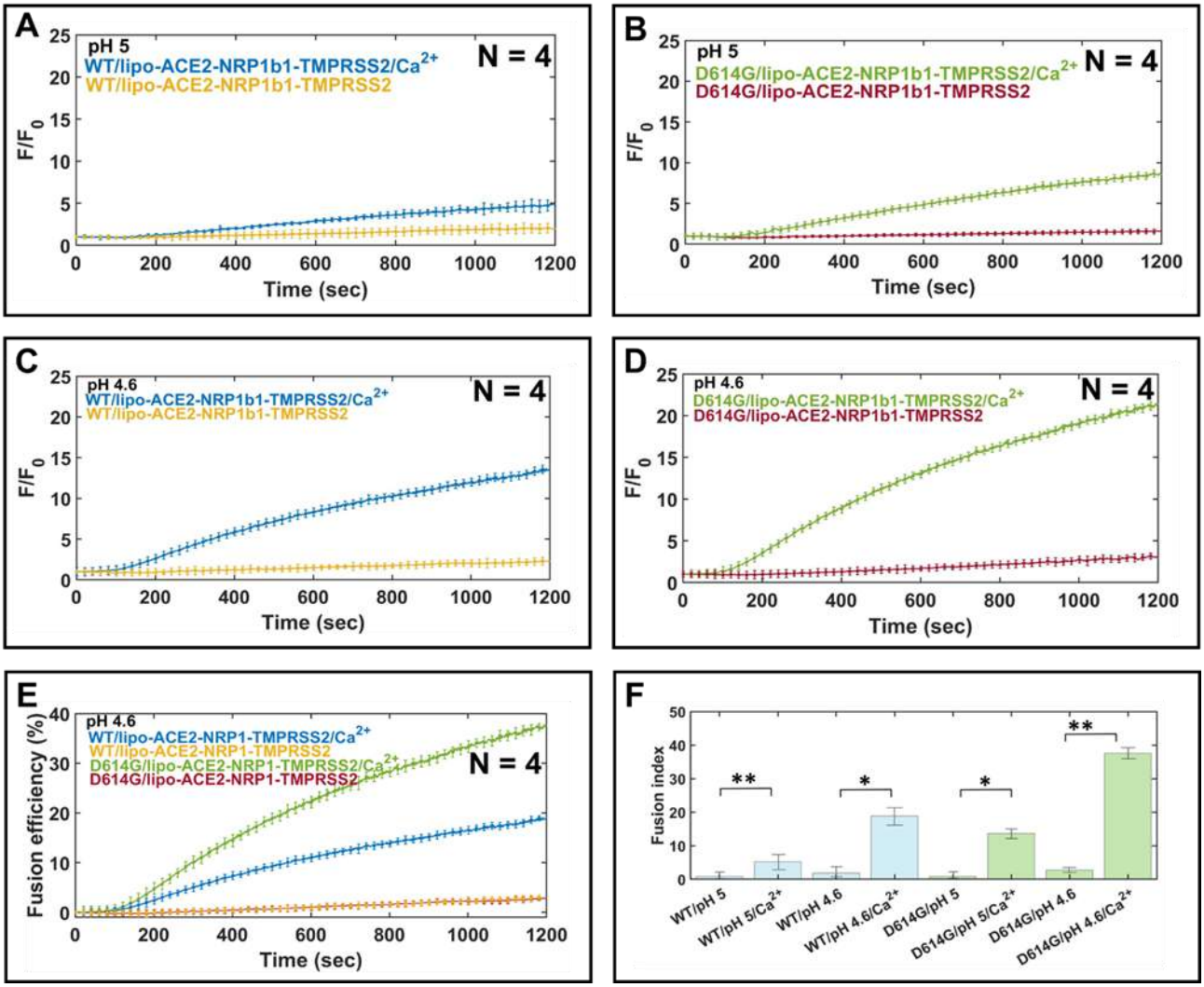

Figure 3: Fluorescence versus time plots for WT (A & C) and D614G (B & D) at pH 5 and pH 4.6 in presence and absence of calcium. Fusion efficiency plot (E) at pH 4.6 in presence and absence of calcium for wild type and D614G pseudotypes. Fusion index (F) for comparison of fusion efficiencies at pH 5 and pH 4.6

b. The infectivity of wild type and D614G virions is abrogated if intracellular calcium is chelated

Before proceeding with further experiments, it was relevant to assess the infectivity of the pseudovirions produced, in order to establish the physiological relevance of the assay results. Hence, the beta-lactamase based enzymatic fusogenicity assay (Figure 4) was performed. The assay involves pseudovirions expressing BlaM-Vpr. HEK293T/17 cells expressing full-length ACE2 or/and NRP1 or/and TMPRSS2 were used as target cells for infectivity.

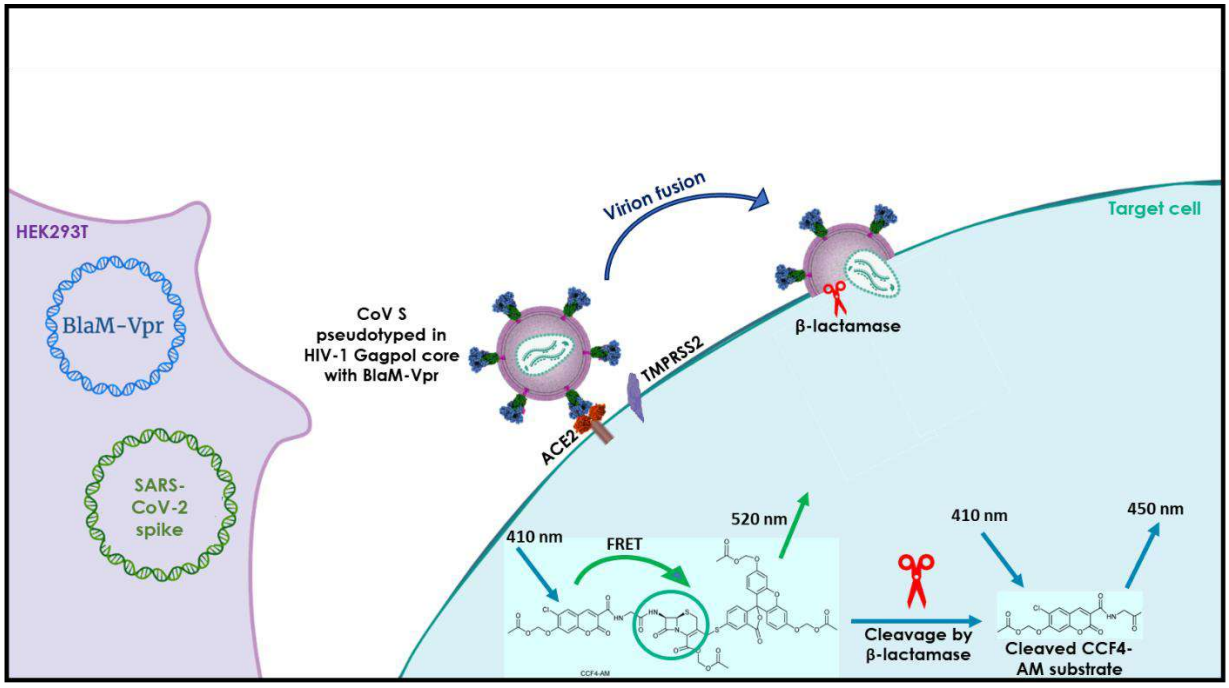

Figure 4: BlaM assay design for monitoring fusogenicity of pseudovirions to the target cell. Assay has been described in detail in the methods section.

The chelator of calcium ion, cell-permeable calcium chelator 1,2-bis(2-aminophenoxy)ethane- N,N,N'N'- tetraacetic acid tetrakis (BAPTA-AM) was used in order to probe the effect of intracellular calcium. As can be observed from the fusogenicity data below, when all the three receptors are present in the cell, the viral entry and fusogenicity is the highest. The presence of BAPTA-AM completely abrogated the viral fusogenicity to the cells, even in the presence of all receptors (Figure 5).

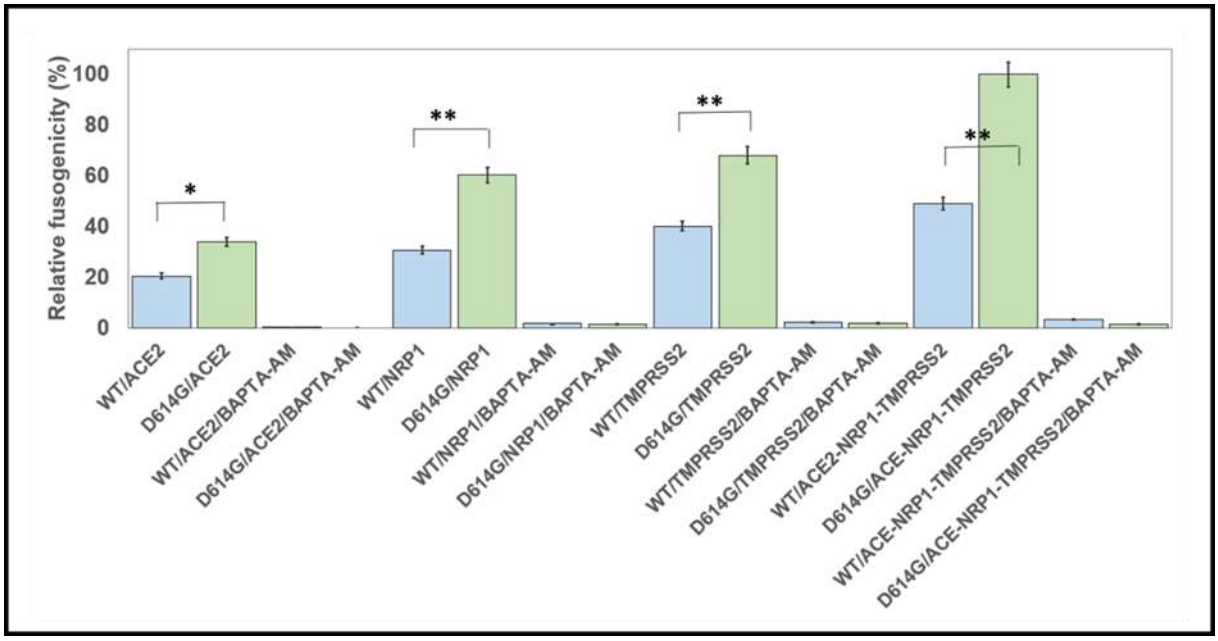

Figure 5: BlaM-based fusogenicity data for different scenarios, in presence and absence of BAPTA-AM.

c. Drugs that block calcium ion channels affect the fusogenicity of SARS-CoV-2 to the target cells

We sought to understand the effect of two calcium ion channel blockers, tetrandrine and verapamil. Both these drugs inhibit calcium release by NAADP (nicotinic acid adenine dinucleotide phosphate) stimulation. The TPCs are stimulated by NAADP to release calcium from endosomes and lysosomes.

The effect of the two drugs on fusogenicity of wild type and D614G pseudovirions was accessed by the BLaM assay. A varying concentration of each drug was used to find out the highest concentration at which the fusogenicity is the least. Tetrandrine was used at a concentration ranging from 0 μM – 6 μM, while verapamil, from 0 μM – 500 μM. Remarkably, for the wild type strain, a sudden drop in fusogenicity was observed when the drug concentration was increased (Figure 6 A, B), while for D614G strain, a gradual decrease in fusogenicity was observed when the drug concentration was increased (Figure 6 A,B). In case of tetrandrine, the most inhibitory concentration was observed to be around 6 μM, while for verapamil, it was observed to be around 500 μM.

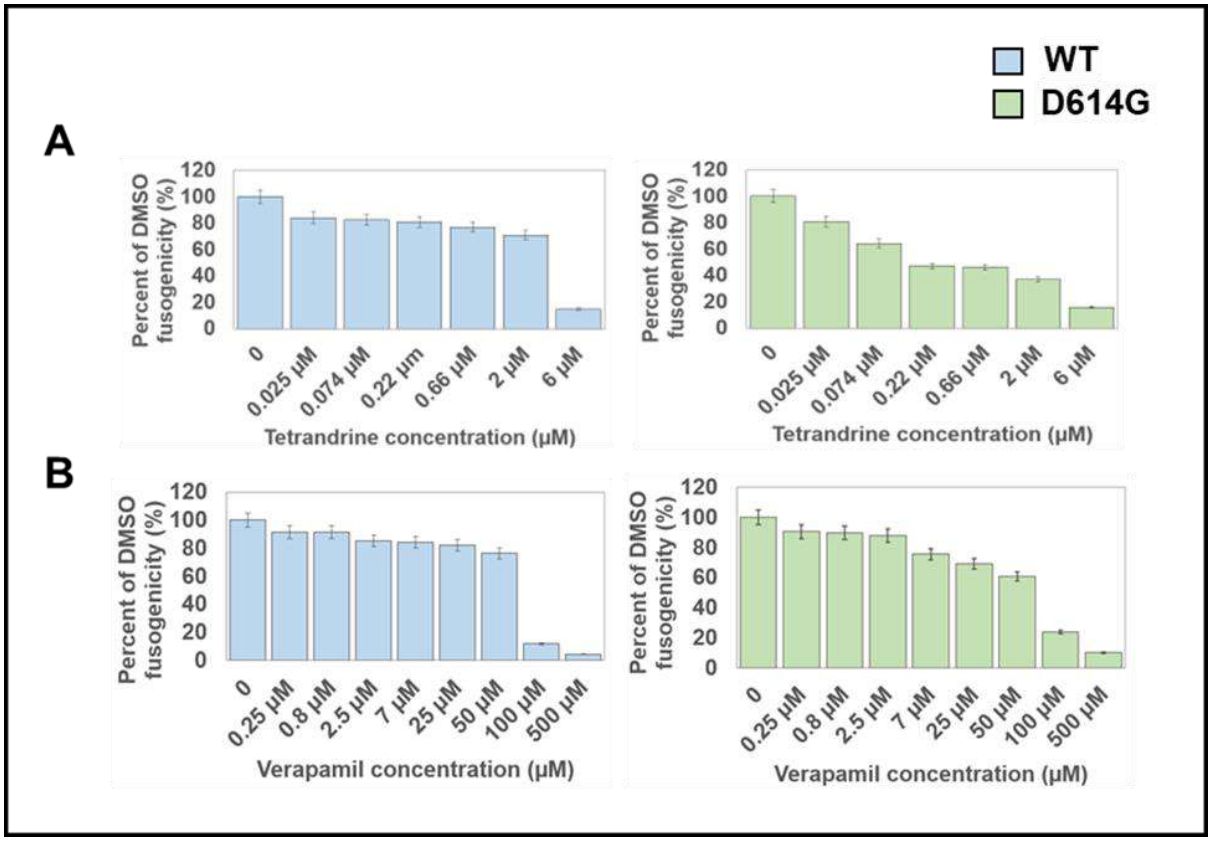

Figure 6: Effect of calcium ion channel blockers tertrandrine (A) and verapamil (B) on the fusogenicity of wild type and D614G strain pseudovirions.

d. D614G-spike membrane fusion is highly sensitive to calcium ion concentration

Since the calcium concentration in the cell varies, a calcium titration was performed to find out if there is any specific calcium concentration at which the fusion efficiency of SARS-CoV-2 is the highest. The titration was initially performed for wild type and D614G strains, at calcium concentrations ranging from 100 µM – 10 mM. Surprisingly, for both the strains, the highest fusogenicity was observed at around 500 µM calcium concentration (Fig 7 A, B), below or above which, the fusogenicity dropped. D614G displayed 2-fold more fusion efficiency as compared to wild type (Figure 7 C) at 500 µM calcium, in presence of pH 4.6. This dynamic nature of the SARS-CoV-2 spike in acting as a calcium sensor came out to be absolutely striking, as increasing calcium concentration decreased the efficiency. From this calcium titration assay, it was concluded that 500 µM calcium is the optimal calcium concentration for fusion to take place. Another noteworthy point at this juncture is that the calcium concentration in endosomes is also around 500-600 µM.

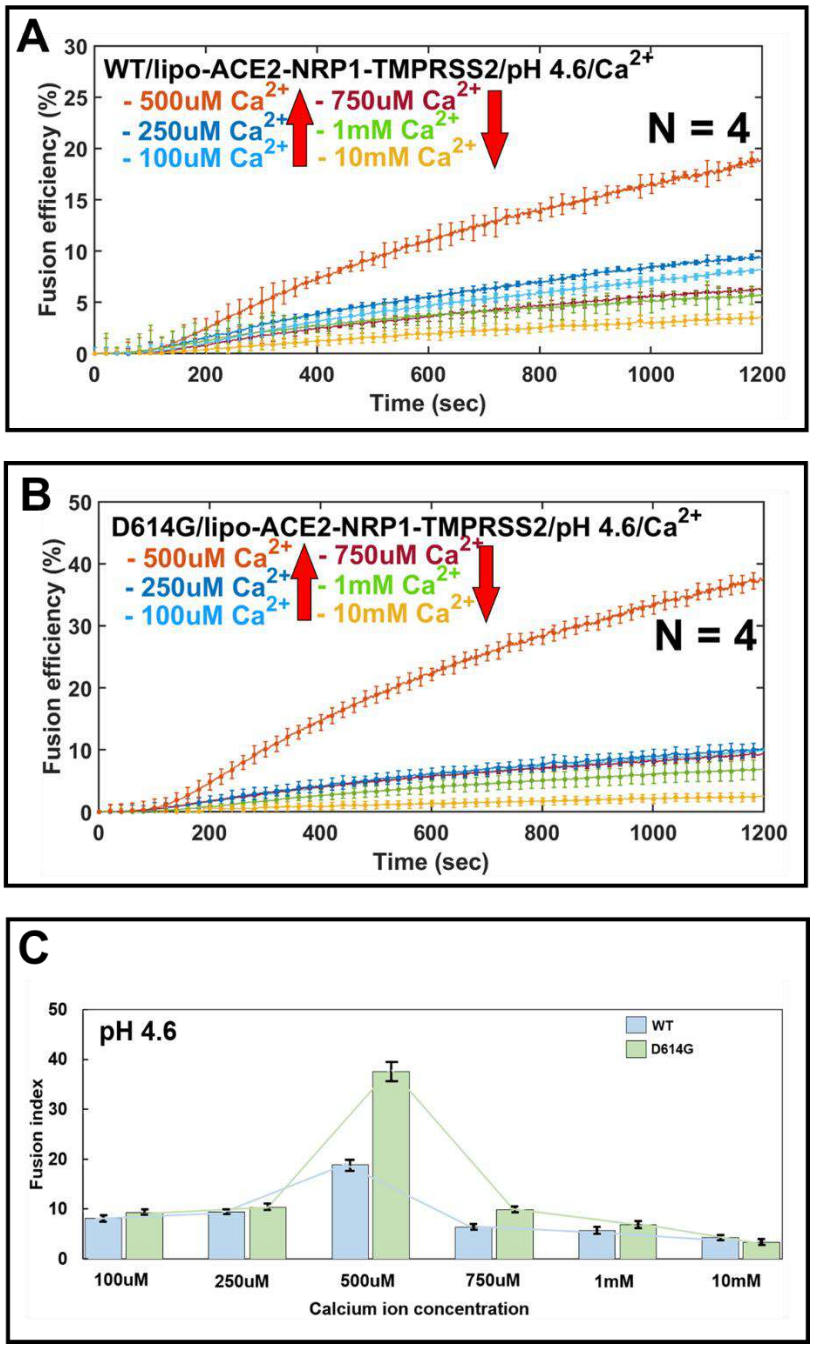

Figure 7: Fusion efficiencies at varying calcium concentrations for the wild type (A) and D614G (B) spike strains. Fusion index (C) comparing the fusion efficiencies at different calcium concentrations for the wild type and the D614G spike.

e. Dynamic calcium sensitivity of the SARS-CoV-2 spike is conserved across different strains

As the dependence of calcium concentration was observed in wild type and D614G strains, we were curious to know the effect of calcium concentrations on other strains. Hence, calcium titration using the fusion assay was performed for the B.1.351 (alpha),

B.1.1.7 (beta), and B.1.617.2 (delta) strains (Figure 8 A-C). The other three strains also showed similar trend as what was observed for wild type and D614G strains. Strikingly, at 500 µM calcium concentration in presence of pH 4.6, the highest fusion efficiency was observed for the B.1.617.2 strain (~ 90-95%), followed by the B.1.1.7 strain (~ 55-60%), and the B.1.351 strain (~ 50-55%) (Figure 8 A-C). All these efficiences are higher than those observed for wild type and D614G, indicating towards the fact that the spike glycoprotein of evolved strains is a more sensitive calcium sensor.

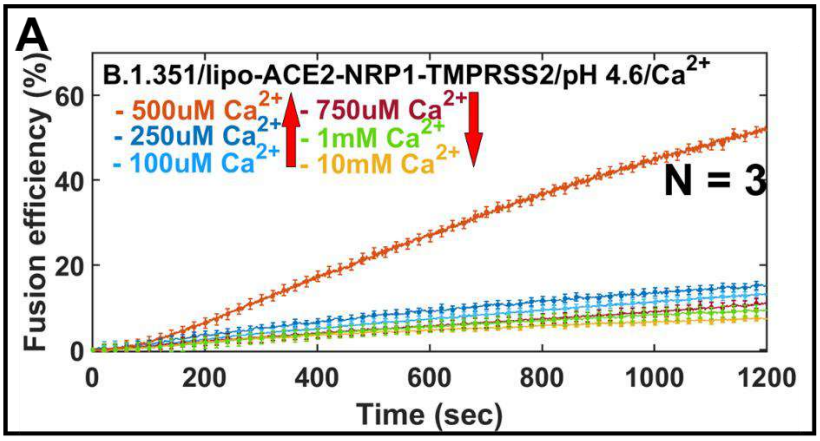

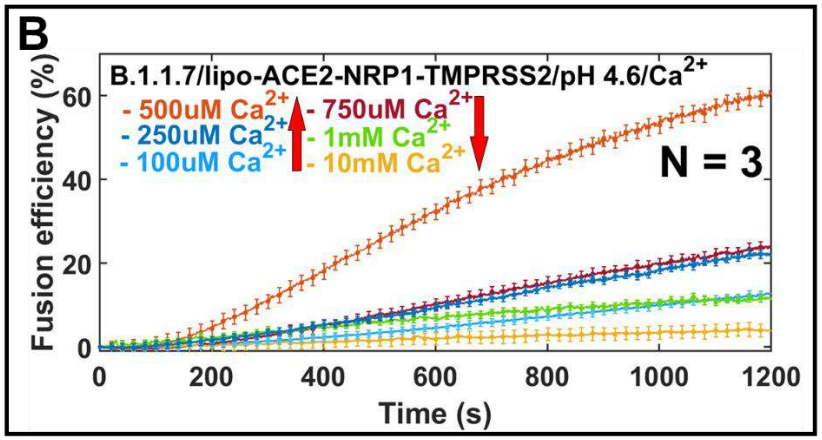

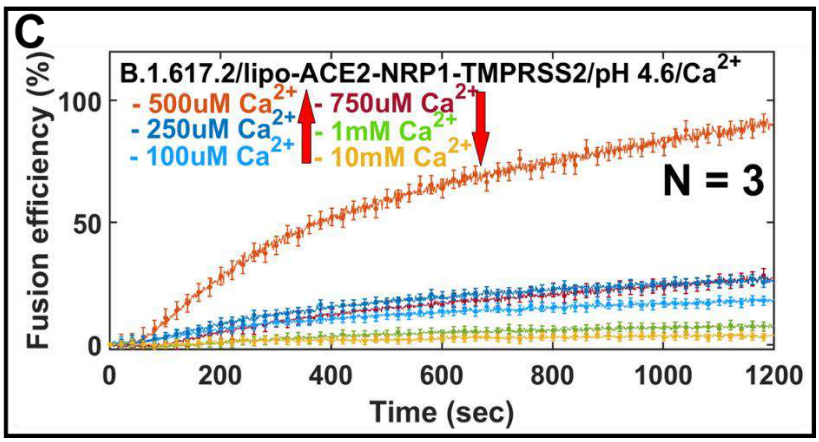

Figure 8: Fusion efficiencies at varying calcium concentrations for the B.1.351 (A), B.1.1.7 (B) and B.1.617.2 (C) spike strains.

When the calcium titration data for all the five strains was compared, it was evident that the spike of B.1.617.2 strain is the most dynamic calcium sensor (Figure 9). From the graph, it can be observed that the nature of calcium concentration dependence is non-monotonic. Even with the non-monotonic nature for all the strains, the B.1.617.2 strain shows more sensitivity at different concentrations of calcium, as compared to the other strains. The decrease in efficiency from 500 µM calcium to 750 µM calcium is abrupt, however, the efficiencies are almost similar at 1 mM and 10 mM.

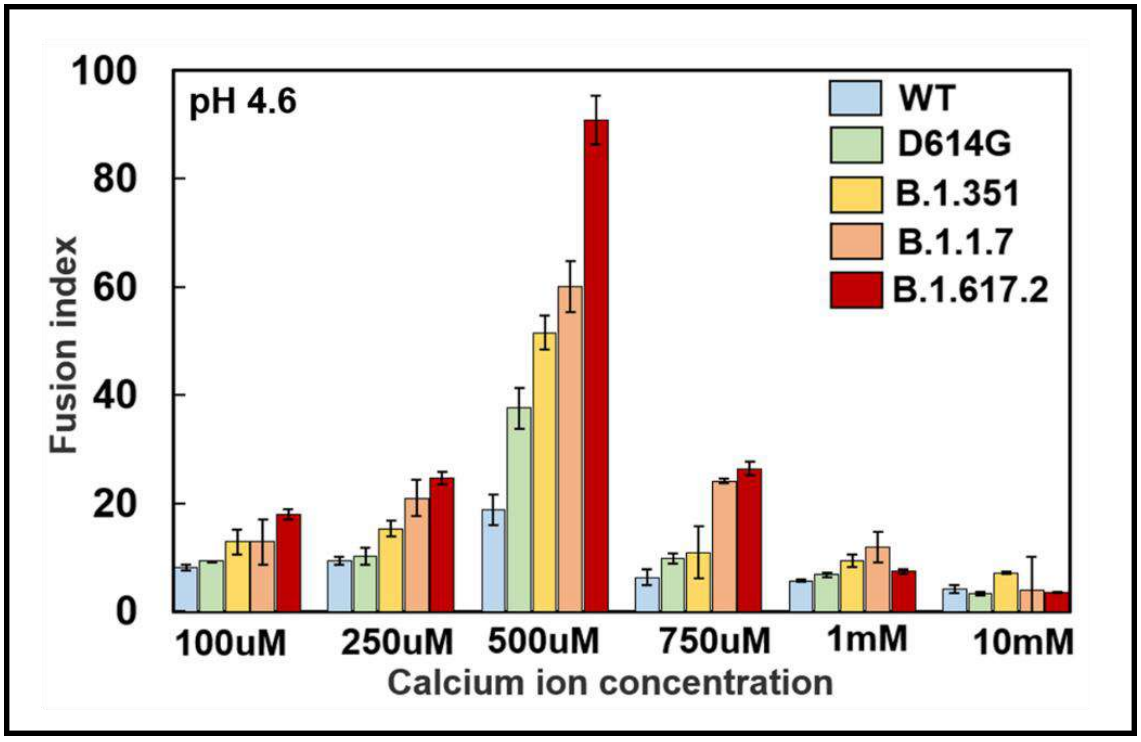

Figure 9: Fusion index comparing the fusion efficiencies at different calcium concentrations for different spike strains of SARS-CoV-2.

f. Calcium directs fusion peptide insertion into the host membrane

An anisotropy assay was designed to understand if calcium is resulting in the insertion of the spike in the host membrane, in order to measure the extent of polarisation of the spike glycoprotein. The 836th position in the fusion peptide proximal region (FPPR) was chosen to tag the Cy3 dye molecule. This region was chosen because it is the region interacting with the host factors during fusion. The fusion peptide itself was not perturbed to ensure that no discrepancies result from the assay. Anisotropy

measurements were then performed to find out the orientations of the spike in different conditions (Figure 10).

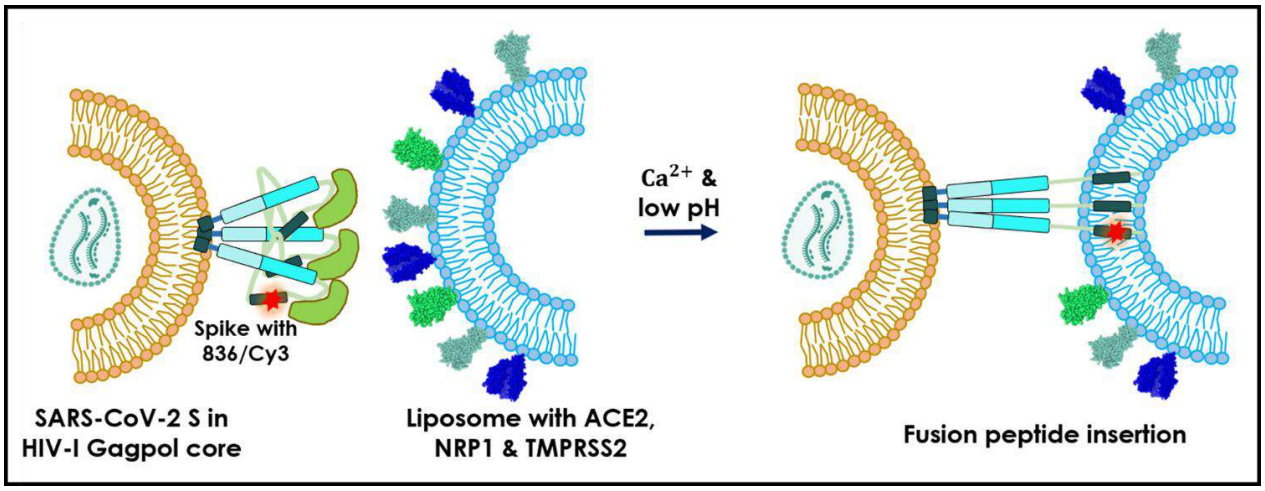

Figure 10: Anisotropy assay design for the SARS-CoV-2 spike. Assay has been described in detail in the methods section.

If the spike is free, no change in anisotropy value would be observed. However, if the spike is bound to a target membrane, it will be oriented in a specific direction, and a change in anisotropy will be seen. We performed the assay with both the wild type and the D614G strains, and observed that at as soon as 500 μM calcium (in presence of pH 4.6) is added at 150 seconds, a sudden jump in anisotropy was seen (Figure 11 A, B). However, no change in anisotropy was seen when a solution without any calcium is added to pH 4.6.

The anisotropy assay was performed for different concentrations of calcium, ranging from 100 μM to 10 mM, and the relative percentage of binding was calculated (Figure 11 C). The highest percentage of binding was seen at 500 μM calcium, and D614G showed higher binding efficiency than wild type.

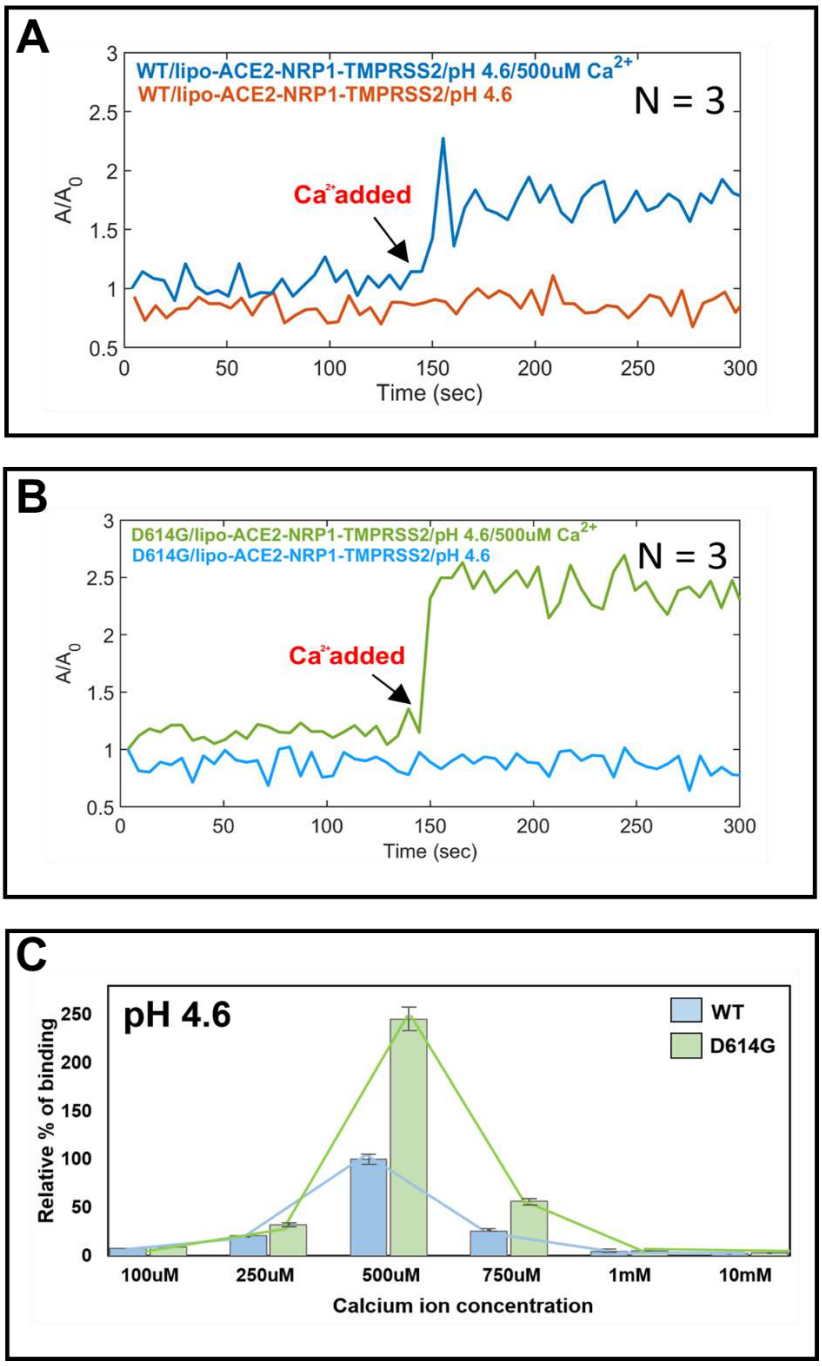

Figure 11: Anisotropy data for the wild type spike (A), and the D614G spike (B) in presence and absence of calcium. Graph (C) showing relative percentage of binding at different calcium concentrations for the wild type and the D614G spike strains.

g. Calcium leads to pre-to-post fusion conformational change of the spike

A Forster resonance energy transfer (FRET) assay was designed to monitor the change in conformation while fusion takes place (Figure 12). Cy3 and Cy5 were used as the FRET pair, where Cy3 would act as the donor, and Cy5 as the acceptor. The

change in FRET states as a function of distance between the dye pair would help in analysing the change in pre-to-post fusion conformation.

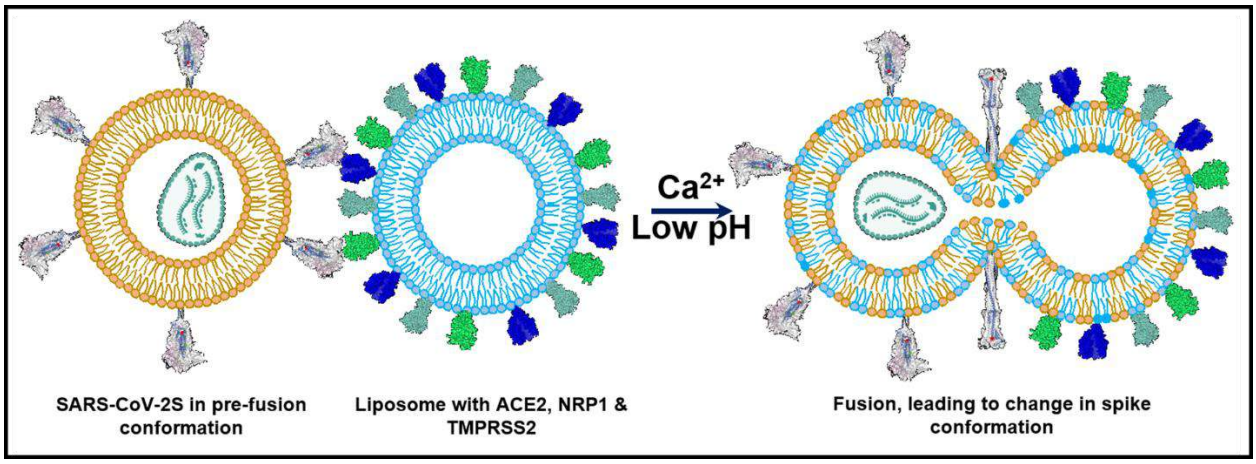

Figure 12: Bulk FRET assay for monitoring the pre-to-post fusion conformational change of the spike. Assay has been described in detail in the methods section.

The positions 836 and 1035 in the spike glycoprotein were used to tag the FRET pair (Figure 13). The positions were first mutated into amber stop codons, and the position was tagged with the non-classical amino acid TCO*A. The dye molecules were then tagged to the non-classical amino acid using the SPIEDAC click chemistry reaction. When the spike is in pre-fusion conformation, the two positions would be closer, and it would give a low FRET state. However, if the spike is in post-fusion conformation, the two positions would be farther, and it would give a high FRET.

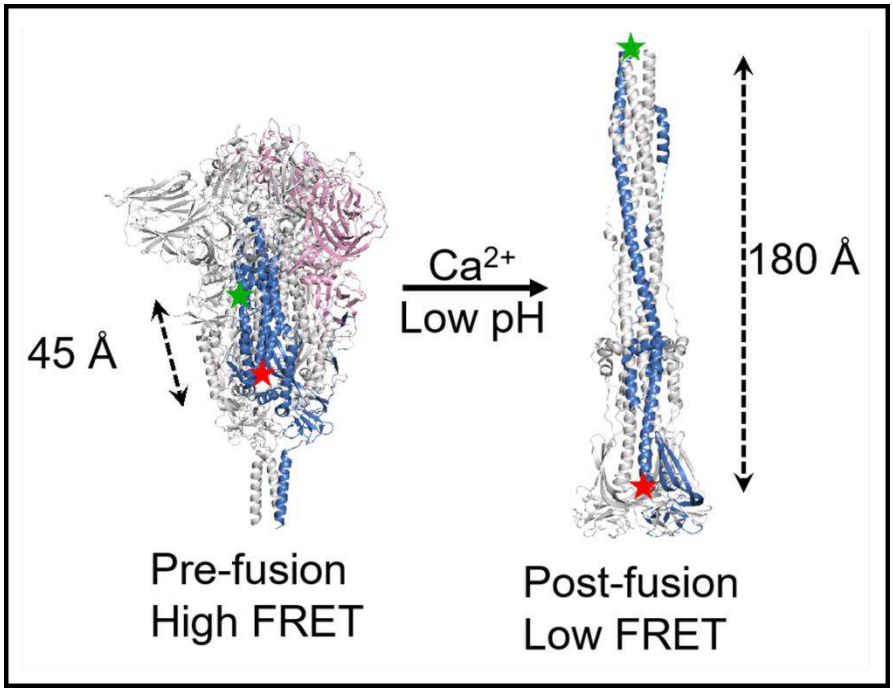

Figure 13: Positions (amino acid residues) chosen for FRET assay. 836 and 1035 positions in the spike protein were chosen in order to tag the donor and acceptor fluorophores and to monitor the pre-to-post fusion conformational change.

Before performing the FRET assay, it was important to ensure that the spike with two dye molecules tagged to it is functional or not. For that purpose, we performed the fusion assay by pseudotyping the $S^{**Cy3/Cy5}$ spike, for both wild type and D614G strains (Figure 14 A, B). The fusion efficiency of the mutant spikes did not drop significantly, as compared to the non-mutant spike. BLaM assay to access the relative fusogenicity to the host cells was also performed (Figure 14 C, D), and no significant dip in fusogenicity was observed. These results prove that the mutant spike is functional.

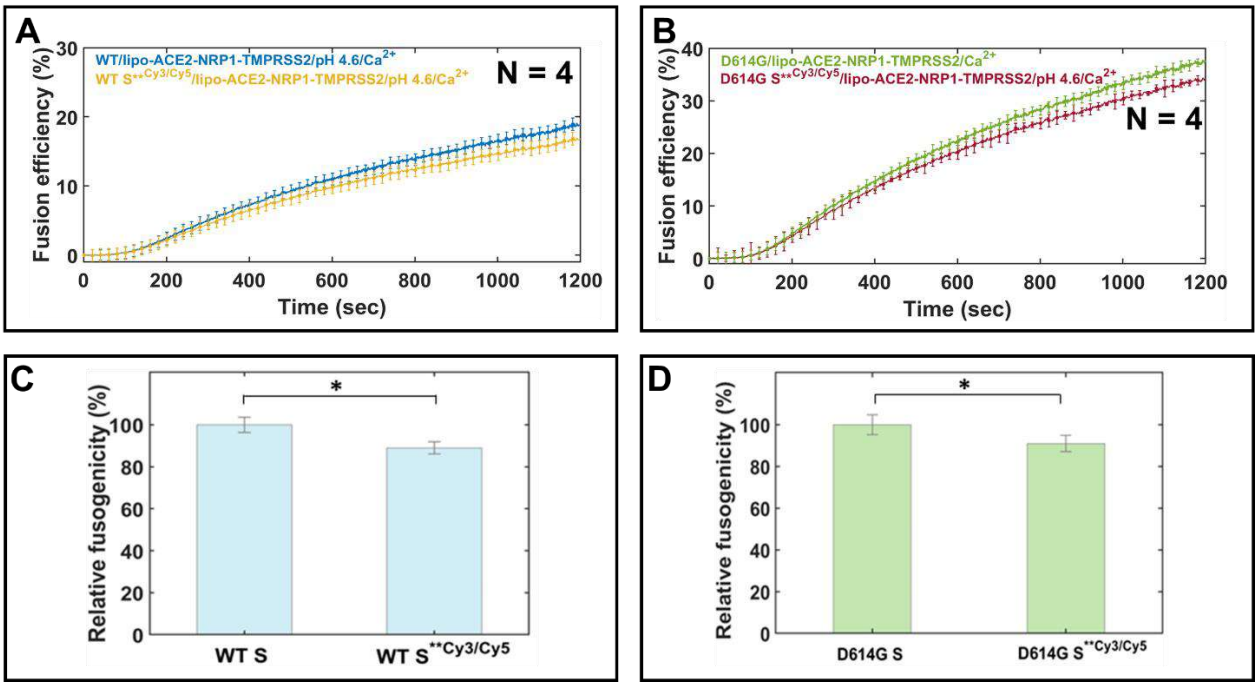

Figure 14: Fusion efficiencies for the wild type (A) and D614G (B) spike strains in presence and absence of fluorophore tags. Relative fusogenicities assessed by BlaM assay for the wild type (C) and D614G (D) spike strains in presence and absence of fluorophore tags.

The FRET assay was first carried out first at pH 4.6, and then at pH 4.6 with 500 μM calcium. For pH 4.6, the majority of the population was observed to be in a pre-fusion conformation (green curve in Figure 15 A, B). At pH 4.6 and 500 μM calcium, most of the spike population was observed to in post-fusion conformation (blue curve in Figure 15 A, B).

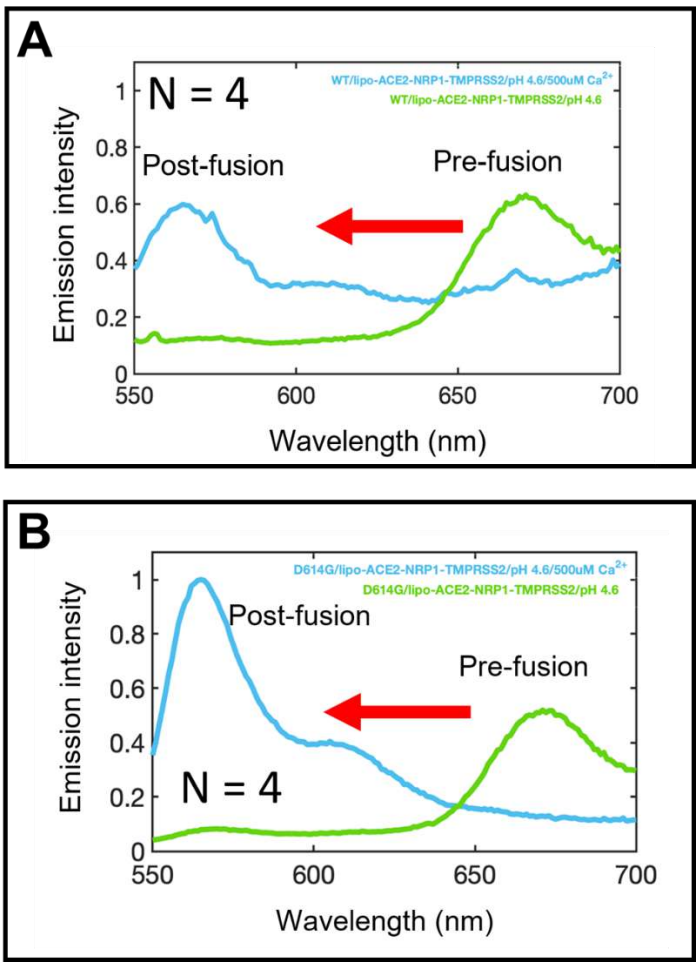

Figure 15: Emission intensity scan for the wild type (A) and D614G (B) spike strains to monitor pre to post fusion conformational dynamics. The acceptor emission is higher during the pre-fusion state, while the donor emission is higher during the post-fusion emission.

Statistical Analysis

Statistical analyses within the scope of our investigation were executed employing the Student's t-test methodology, with comprehensive elucidations provided in the corresponding figure captions. Each experiment was performed four times (N=4) in order to ensure that no experimental or assessment bias arises. The error bar for each dataset represents standard error of mean. The computation of p-values was conducted via the two-tailed Student's t-test. Instances where the p-values fell below 0.0001 were denoted by an asterisk (*), while instances with p-values below 0.00001 were designated by a double asterisk (**), consistently upheld throughout the entire duration of our study.

Discussion

This study has developed a fusion assay for detection of SARS-CoV-2 fusion in a robust and efficient manner. The assay can be used to find out the individual factors which affect the fusion of the virion to the host cell. The fusion assay that has been standardized through this work is novel and will help in easy detection of the triggering factors. The assay helped in pinpointing that even when ACE2 is the actual receptor for SARS-CoV-2 spike, fusion can also take place independently of ACE2, if other factors which can engage with the spike are present in a conducive environment, with optimal conditions.

It was remarkable to observe that the most optimal fusion was seen at late endosomal pH with endosomal concentration of calcium. This observation indicates that low pH is crucial for bringing about important conformational changes in the spike, and calcium may be helping in stabilising the pre-to-post fusion conformational rearrangement. Even when the spike is able to recognise and interact with ACE2, NRP1 and TMPRSS2 at the cell membrane, our data shows that the final post-fusion conformational rearrangement happens in the late endosomes when the optimal pH and calcium concentration are reached.

On the basis of the dependence of fusion on calcium concentration that has been witnessed, a working model has been proposed (Figure 16). There is a gradient of calcium concentration which the virion would encounter while moving from the extracellular to the lysosomal environment According to this model, when the calcium concentration is very low, for example, as in the cytosol, the spike cannot undergo the requisite conformational changes to go to a thermodynamically stable post-fusion conformation. When the calcium concentration is high, as at the extracellular plasma membrane level, even then the spike cannot achieve a post fusion conformation. However, the mechanism which is followed by the spike in an environment of high calcium concentration needs to be explored; it may be because of insertional inactivation, or it may be that a stable conformation cannot be formed. When the calcium concentration is optimal, around 500 μM, as is what is found in the lysosomes, or late endosomes, then only can the spike achieve a stable post fusion conformation, leading to fusion of the virion to the target membrane.

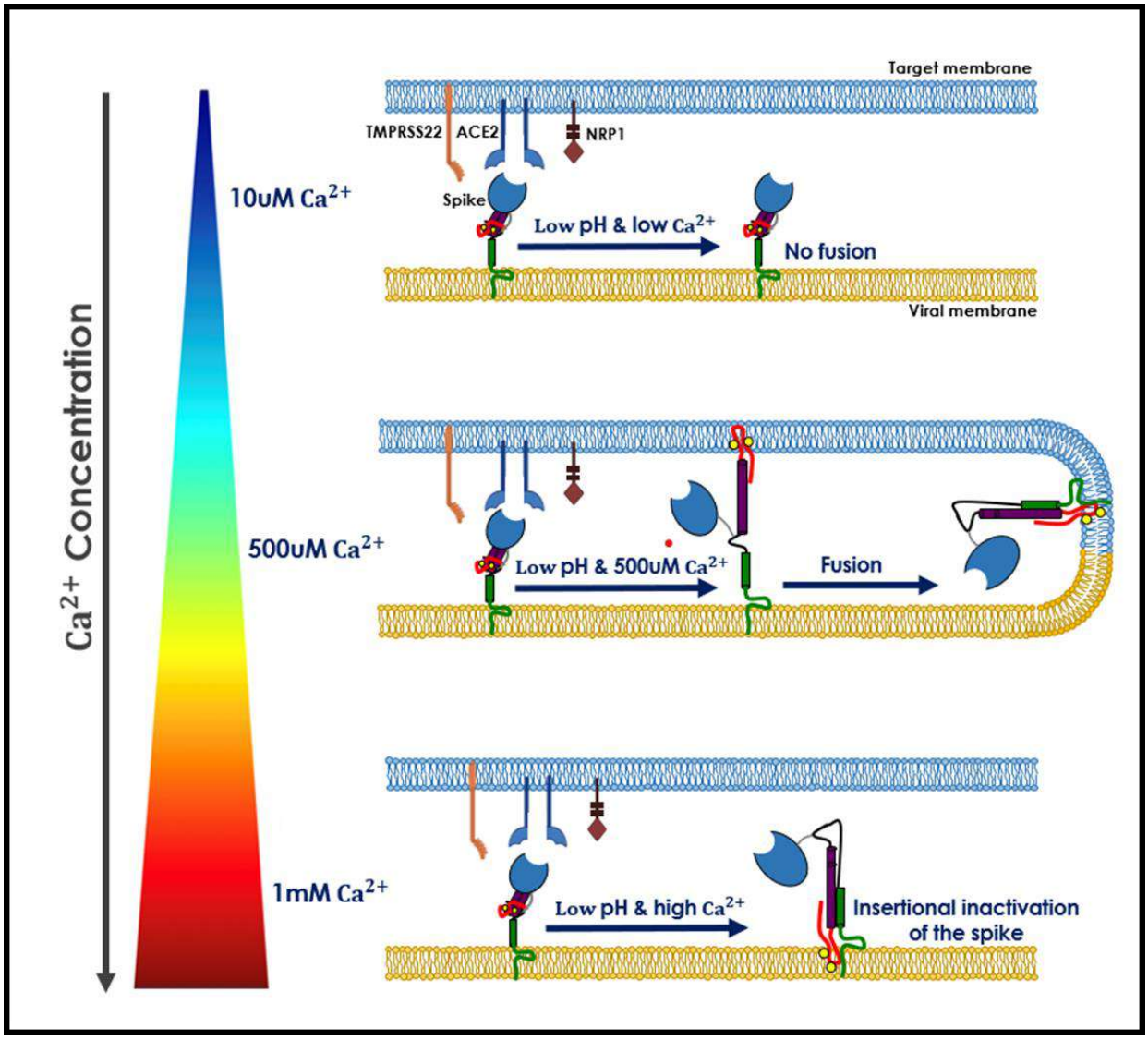

Figure 16: Proposed model for the optimal conditions required for SARS-CoV-2 fusion.

If we look at the actual picture, some amount of fusion may be taking place at the plasma membrane as well, but the fusion kinetics may be extremely slow to be followed by our fusion assays. Hence, the endo-lysosomal medium of entry may be the preferred mode of entry for the SARS-CoV-2 coronavirus. Previous studies also point towards the same, however, none of the studies delineated the role of calcium.

Another important conclusion from this work is the enhanced sensitivity of evolved spike variants towards calcium. It is really remarkable how the spike of more evolved variants, i.e. the ones with more mutations than the wild type, may have evolved at better calcium sensing. The data of the calcium titration with different variants corroborates with the fact that the B.1.617.2 strain is more infectious and fusogenic than any other strain. While calcium ions may be binding to the negatively charged

aspartic acid residues, the presence of different mutations in the spike of variant strains may be affecting the manner in which calcium is binding to the negatively charged aspartic acid residues.

Impact of the research in the advancement of knowledge or benefit to mankind

Before our story was published, it was not clear in the field as to which is the preferred mode of fusion for the virus: the membrane or the endosomal pathway. Our study established that it is the endosomal pathway which the coronavirus uses for fusion, and that fusion can take place only when acidic pH and calcium are present. This discovery about the role of calcium is monumental, as this is the first time that a study has shown that calcium can interact directly with the coronavirus spike. Through our assays, we proved that without calcium, the important structural rearrangements that are needed for fusion cannot take place.

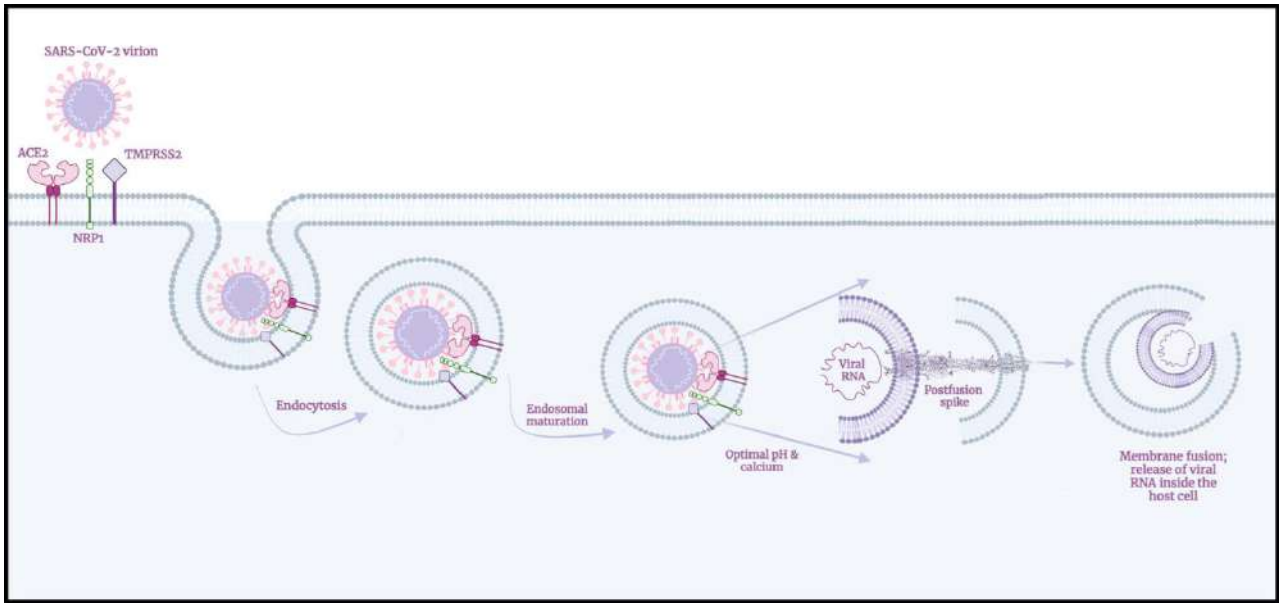

Figure 17: Physiological model for SARS-CoV-2 entry into host cell

Now that the role of calcium is established in coronavirus biology, the next prudent question would be: so what if calcium interacts with the spike? Does this knowledge help us in designing any therapeutic strategies? To answer with brevity, we would say, yes. Though we are not at the advanced stage of clinical trials yet, but we tried treating the cells with some drugs which block the entry of calcium inside the cell, and then tried assessing the entry of SARS-CoV-2 virions, and voila, we found that at a specific concentration, the entry is entirely restricted! This paves the way for future clinical

research on how these kinds of drugs can be used for combating coronavirus infection. But the one necessary thing that this research has done, is to help us all appreciate the elegance and the beauty with which natural processes have evolved. Nothing is random in nature, no matter if it's a new virus or a century old virus. All processes are, after all, as Wordsworth would say, "*bound each to each by natural piety*".

Literature references

• Lai AL, Millet JK, Daniel S, Freed JH, Whittaker GR. The SARS-CoV Fusion Peptide Forms 757 an Extended Bipartite Fusion Platform that Perturbs Membrane Order in a Calcium

-Dependent 758 Manner. J Mol Biol. 2017;429(24):3875-92.

• Khelashvili G, Plante A, Doctorate M, Weinstein H. Ca(2+)-dependent mechanism of membrane insertion and destabilization by the SARS-CoV-2 fusion peptide. Biophys J. 2021;120(6):1105-19.

• Koppisetti RK, Fulcher YG, Van Doren SR. Fusion Peptide of SARS-CoV-2 Spike 810 Rearranges into a Wedge Inserted in Bilayered Micelles. J Am Chem Soc. 2021;143(33):13205- 11

• Lim, S.; Zhang, M.; Chang, T.L. ACE2-Independent Alternative Receptors for SARS-CoV-2. Viruses 2022, 14, 2535. https://doi.org/10.3390/v14112535

• Kexin Yan and others, Evolution of ACE2-independent SARS-CoV-2 infection and mouse adaption after passage in cells expressing human and mouse ACE2, Virus Evolution, Volume 8, Issue 2, 2022, veac063, https://doi.org/10.1093/ve/veac063

• Shen, XR., Geng, R., Li, Q. et al. ACE2-independent infection of T lymphocytes by SARS-CoV-2. Sig Transduct Target Ther 7, 83 (2022). https://doi.org/10.1038/s41392-022-00919-x

• Daly, J.L., Simonetti, B., Klein, K., Chen, K.-E., Williamson, M.K., Anto´ n-Pla´-garo, C., Shoemark, D.K., Simo´ n-Gracia, L., Bauer, M., Hollandi, R., et al. (2020). Neuropilin-1 is a host factor for SARS-CoV-2 infection. Science 370, 861–865

• H. B. Pang, G. B. Braun, T. Friman, P. Aza-Blanc, M. E. Ruidiaz, K. N. Sugahara, T. Teesalu, E. Ruoslahti, An endocytosis pathway initiated through neuropilin-1 and regulated by nutrient availability. Nat. Commun. 5, 4904 (2014).

• Abigail G GarrityWuyang WangCrystal MD CollierSara A LeveyQiong GaoHaoxing Xu (2016) The endoplasmic reticulum, not the pH gradient, drives calcium refilling of lysosomes eLife 5:e15887.

• Burkard, C., Verheije, M.H., Wicht, O., van Kasteren, S.I., van Kuppeveld, F.J., Haagmans, B.L., Pelkmans, L., Rottier, P.J.M., Bosch, B.J., and de Haan, C.A.M. (2014). Coronavirus cell entry occurs through the endo-/lysosomal pathway in a proteolysis-dependent manner. PLoS Pathog. 10, e1004502.

• Carten et al. bioarchives. It Takes Two: Bimodal interactions between the SARS-CoV-1 fusion peptid and Ca2+ ions promote membrane insertion and viral entry https://doi.org/10.1101/2022.03.03.482731

• X. Ou, Y. Liu, X. Lei, P. Li, D. Mi, L. Ren, L. Guo, R. Guo, T. Chen, J. Hu, Z. Xiang, Z. Mu, X. Chen, J. Chen, K. Hu, Q. Jin, J. Wang, Z. Qian, Characterization of spike glycoprotein of SARS-CoV-2 on virus entry and its immune cross-reactivity with SARS-CoV, Nat. Commun. 11 (2020) 1620, https://doi.org/10.1038/s41467-020-15562-9 (the one with tetrandrine report and studies on endo-lysosomal entry pathway of sars cov 2)

• L. Di Filippo, A.M. Formenti, P. Rovere-Querini, M. Carlucci, C. Conte, F. Ciceri, A. Zangrillo, A. Giustina, Hypocalcemia is highly prevalent and predicts hospitalization in patients with COVID-19, Endocrine 68 (2020) 475–478, https://doi.org/10.1007/s12020-020-02383-5.